Afterburning Predictions for Metal-Modified Propellant Motor Exhausts

D. E. Jensen* and B. C. Webb†
Ministry of Defence, Rocket Propulsion Establishment, Westcott, Aylesbury, Buckinghamshire, England

Predicted extents of afterburning in fuel-rich exhausts of metal-modified, double base propellant rocket motors have been investigated by means of a plume prediction code, which incorporates fully coupled turbulent kinetic energy boundary-layer and nonequilibrium chemical reaction schemes. The influences of a number of metals, including potassium, iron, molybdenum, tungsten, barium, tin, and chromium, on afterburning have been examined for a 300 N thrust motor. The effects of changes in total effluent mass flow rate and exit temperature were determined for both modified and unmodified propellants under static and flight conditions at sea level.

I. Introduction

ELECTROMAGNETIC and other properties of rocket exhaust plumes depend strongly upon whether or not afterburning (secondary combustion) of fuel-rich products – principally CO and H_2 – of propellant combustion occurs. Afterburning takes place when the sequence of chain-branching chemical reactions

$$H + O_2 \rightarrow OH + O \quad (1)$$

$$O + H_2 \rightarrow OH + H \quad (2)$$

and

$$OH + H_2 \rightarrow H_2O + H \quad (3)$$

produces active free radicals like H, OH, and O faster than these radicals can be removed by the chain termination processes of mixing and such slow chemical recombinations, aided by energy-removing collision partners M, as

$$H + H + M \rightarrow H_2 + M \quad (4)$$

and

$$H + OH + M \rightarrow H_2O + M \quad (5)$$

The burning of carbon monoxide, which takes place concurrently with that of hydrogen, tends to propagate the combustion sequence rather than to result in net production or removal of radicals because the principal reaction controlling the oxidation of CO

$$CO + OH \rightarrow CO_2 + H \quad (6)$$

simply replaces one active radical by another.

Certain metals are known to cause accelerated radical removal in laboratory flames, and interpretations of these effects in terms of chemical reaction rates have recently been offered.[1-4] The purpose of this paper is to describe predicted effects of selected metal-containing additives upon exhaust afterburning, and in particular to investigate whether these additives are expected to accelerate radical removal sufficiently to prevent secondary combustion taking place in circumstances where it does so in the absence of additives. Interest centers on metals present in typical ballistic modifiers, and on other metals which appear to be promising afterburning suppression candidates. A program of measurements designed to test the predictions under conditions of practical rocket motors is in progress at the Rocket Propulsion Establishment.

Received September 12, 1975. Presented as Paper 75-1232 at the AIAA/SAE 11th Propulsion Conference, Anaheim, Calif., September 29-October 1, 1975.

Index categories: Reactive Flows; Combustion in Gases; Solid and Hybrid Rocket Engines.

*Head, Applied Combustion Section.

†Member, Applied Combustion Section.

II. Combustion Suppression Mechanisms

Potassium

Alkali metals have been used as combustion inhibitors in various practical contexts, and a qualitative interpretation of the mode of action of potassium has been given by Rosser, Inami, and Wise[5] and Friedman and Levy,[6] in terms of the reaction sequence

$$KOH + H \rightarrow K + H_2O \quad (7)$$

$$K + OH + M \rightarrow KOH + M \quad (8)$$

(net effect $H + OH \rightarrow H_2O$, acceleration of chain termination and hence combustion suppression). Reaction (8) is itself a three-body reaction, of course, but what scanty experimental evidence is available on this reaction[7] suggests that it may provide faster recombination than do reactions (4) and (5) under the experimental conditions of interest. This type of mechanism is also favored, for rocket exhaust flame conditions, by McHale.[8] The mechanism adopted here consists of reactions (7) and (8), with the rate coefficients and uncertainty factors listed in Table 1.

In practice, combustion suppression by potassium suffers from the disadvantage that the suppressed flames tend to produce excessive secondary smoke: indeed, this is one of the factors that led to the search for alternative suppressors.

Iron

The suggested cycle of reactions[3]

$$FeOH + H \rightarrow FeO + H_2 \quad (9)$$

$$FeO + H_2O \rightarrow Fe(OH)_2 \quad (10)$$

and

$$Fe(OH)_2 + H \rightarrow FeOH + H_2O \quad (11)$$

(net effect $H + H \rightarrow H_2$, occurring through relatively fast bimolecular steps), together with the reaction[3]

$$FeOH + H \rightarrow Fe + H_2O \quad (12)$$

is adopted here as the mechanism of combustion inhibition by iron. The rate coefficients and uncertainty factors for reactions (9-12) are listed in Table 1. Thermochemical data for the species involved are taken from Refs. 9 and 10.

Molybdenum

The mechanism through which molybdenum additives catalyze radical removal is taken from Ref. 4. It consists of the three relatively rapid bimolecular reactions

$$HMoO_3 + H \rightarrow MoO_3 + H_2 \quad (13)$$

$$MoO_3 + H_2O \rightarrow H_2MoO_4 \quad (14)$$

and

$$H_2MoO_4 + H \rightarrow HMoO_3 + H_2O \quad (15)$$

(net effect again $H + H \rightarrow H_2$), with rate coefficients listed in Table 1 and thermochemical data from Refs. 4 and 9. There are substantial uncertainties in the thermochemical data for $HMoO_3$ as well as in the rate coefficients.

Tungsten

The suppression mechanism for tungsten[4] analogous to that for molybdenum, consists of the reactions

$$HWO_3 + H \rightarrow WO_3 + H_2 \quad (16)$$

$$WO_3 + H_2O \rightarrow H_2WO_4 \quad (17)$$

and

$$H_2WO_4 + H \rightarrow HWO_3 + H_2O \quad (18)$$

with rate coefficients and uncertainty factors listed in Table 1 and thermochemical data from Refs. 4 and 9.

Barium

The reactions included to account for catalysis of radical recombination by barium are

$$BaOH + H \rightarrow BaO + H_2 \quad (19)$$

$$BaO + H_2O \rightarrow Ba(OH)_2 \quad (20)$$

$$Ba(OH)_2 + H \rightarrow BaOH + H_2O \quad (21)$$

and

$$BaOH + H \rightarrow Ba + H_2O \quad (22)$$

with rate coefficients (Table 1) and thermochemical data from Refs. 1, 9, 12, and 13.

Tin and Chromium

Measurements on the catalytic effects of tin and chromium on radical recombination have been made,[2, 4, 14, 15] but no quantitative mechanism for these metals has yet been fitted to the experimental data. An empirical fit to the measurements on fuel-rich $H_2 + O_2 + N_2$ flames, however, can be represented in terms of the overall reactions

$$H + H + (Sn) \rightarrow H_2 + (Sn) \quad (23)$$

Table 1 Basic combustion and additive mechanism chemical reaction rate coefficients

Reaction	Forward Rate Coefficient[a]	Uncertainty Factor[b]
$O + O + M \rightarrow O_2 + M$	$1 \times 10^{-29} T^{-1}$	30
$O + H + M \rightarrow OH + M$	$1 \times 10^{-29} T^{-1}$	30
$H + H + M \rightarrow H_2 + M$	$5 \times 10^{-29} T^{-1}$	10
$H + OH + M \rightarrow H_2O + M$	$2 \times 10^{-28} T^{-1}$	10
$CO + O + M \rightarrow CO_2 + M$	$1 \times 10^{-29} T^{-1} \exp(-1250/T)$	30
$OH + H_2 \rightarrow H_2O + H$	$3.6 \times 10^{-11} \exp(-2600/T)$	3
$O + H_2 \rightarrow OH + H$	$2.9 \times 10^{-11} \exp(-4730/T)$	3
$H + O_2 \rightarrow OH + O$	$3.7 \times 10^{-10} \exp(-8400(T)$	3
$CO + OH \rightarrow CO_2 + H$	$9 \times 10^{-13} \exp(-540/T)$	5
$OH + OH \rightarrow H_2O + O$	$1.0 \times 10^{-11} \exp(-390/T)$	5
$KOH + H \rightarrow K + H_2O$	$2 \times 10^{-12} \exp(-400/T)$	30
$K + OH + M \rightarrow KOH + M$	$6 \times 10^{-28} T^{-1}$	30
$FeOH + H \rightarrow FeO + H_2$	$5 \times 10^{-11} \exp(-800/T)$	10
$FeO + H_2O \rightarrow Fe(OH)_2$	9×10^{-12}	5
$Fe(OH)_2 + H \rightarrow FeOH + H_2O$	$1.1 \times 10^{-10} \exp(-300/T)$	5
$FeOH + H \rightarrow Fe + H_2O$	$2 \times 10^{-12} \exp(-600/T)$	30
$HMoO_3 + H \rightarrow MoO_3 + H_2$	$1.1 \times 10^{-10} \exp(-1400/T)$	10
$MoO_3 + H_2O \rightarrow H_2MoO_4$	1×10^{-11}	20
$H_2MoO_4 + H \rightarrow HMoO_3 + H_2O$	$1.4 \times 10^{-10} \exp(-300/T)$	20
$HWO_3 + H \rightarrow WO_3 + H_2$	$1.6 \times 10^{-10} \exp(-1000/T)$	10
$WO_3 + H_2O \rightarrow H_2WO_4$	1×10^{-10}	20
$H_2WO_4 + H \rightarrow HWO_3 + H_2O$	$3 \times 10^{-10} \exp(-1000/T)$	20
$BaOH + H \rightarrow BaO + H_2$	$3 \times 10^{-11} \exp(-800/T)$	10
$BaO + H_2O \rightarrow Ba(OH)_2$	3×10^{-12}	10
$Ba(OH)_2 + H \rightarrow BaOH + H_2O$	$1 \times 10^{-10} \exp(-300/T)$	10
$BaOH + H \rightarrow Ba + H_2O$	$2 \times 10^{-12} \exp(-500/T)$	30
$H + H + (Sn) \rightarrow H_2 + (Sn)$	5×10^{-28}	10
$H + H + (Cr) \rightarrow H_2 + (Cr)$	2×10^{-27}	10
$H + Cl_2 \rightarrow HCl + Cl$	$7 \times 10^{-10} \exp(-1500/T)$	5
$Cl + H_2 \rightarrow HCl + H$	$4 \times 10^{-11} \exp(-2200/T)$	10
$H_2O + Cl \rightarrow HCl + OH$	$5 \times 10^{-11} \exp(-9500/T)$	30
$OH + Cl \rightarrow HCl + O$	$3 \times 10^{-11} \exp(-2500/T)$	30
$H + Cl + M \rightarrow HCl + M$	$4 \times 10^{-26} T^{-2}$	100
$Cl + Cl + M \rightarrow Cl_2 + M$	$3 \times 10^{-29} T^{-1}$	30

[a] In ml-molecule-second units.
[b] Defined as in Refs. 7, 11.

Table 2 Effects of particles on radical recombination

Particle Radius, nm	k, ml molecule^{-1} sec^{-1} at 1200 K
10	1.6×10^{-6}
100	1.6×10^{-4}
1000	1.6×10^{-2}
10000	1.6

and

$$H+H+(Cr)\rightarrow H_2+(Cr) \quad (24)$$

where (Sn) and (Cr) denote species (not free atoms, and probably including major contributions from SnO[14] and $HCrO_3$[15] respectively) formed from tin and chromium in the flames. The rates of reactions (23) and (24) may then be written as k_{23} [H]^2 [Sn]$_c$ and k_{24} [H]^2 [Cr]$_c$ respectively, where [Sn]$_c$ and [Cr]$_c$ are the total concentrations of tin and chromium derivatives respectively. This lack of a proper combustion inhibition mechanism makes the interpretation of effects of tin and chromium on afterburning uncertain, because it obscures the temperature and composition dependences of the catalysis. The values of the rate coefficients k_{23} and k_{24} used in the few calculations made on the effects of tin and chromium additives stem from Refs. 2, 4, 14, and 15 and are listed in Table 1.

Chlorine

The effects of the non-metal chlorine on secondary combustion were briefly investigated, for purposes of comparison, because chlorine-containing additives have often been tried as flame inhibitors.[16] The reactions of HCl, Cl, and Cl_2, together with their rate coefficients and associated uncertainty factors, are shown in Table 1.

Consequences of Particle Formation

It is appropriate to consider the implications of a significant proportion of any additive entering the exhaust as condensed particles, for the formation of such particles might be expected both to reduce the magnitude of the homogeneous gas phase catalysis effects, and to permit heterogeneous radical removal. In the latter, the rate-limiting step is likely to be first-order in [H] and determined by the rate of collisions at the particle surfaces.[15] If [P] is the local concentration of additive-containing particles, simple collision theory gives the rate of hydrogen atom removal ([H] >> [OH] and [O]) as

$$-d[H]/dt = k[P][H]$$

$$= 4.6\times10^4 r^2\sqrt{T}\,[P][H] \text{ molecule ml}^{-1}\text{ sec}^{-1} \quad (25)$$

for a sticking probability of unity, where r is the particle radius in cm and T the local exhaust temperature. Values of k for different particle radii are shown in Table 2. Heterogeneous radical removal terms of this type were incorporated in a series of calculations with the computer code described below, in which it was assumed that all the metal-containing additive was present throughout the exhaust in condensed form. These calculations showed that heterogeneous radical removal, although leading to lower free radical concentrations, was not fast enough to cause afterburning suppression even for the smallest assumed particle radius (which maximizes the total available particle surface area for a given mass fraction of additive in the propellant). Rough estimates of heat transfer rates and condensation rates suggest 1) that these additives are likely to volatize in the chamber (c.f. Ref. 8) but 2) that characteristic condensation times may not be as much greater than nozzle residence times for motors of interest. Future work on prediction of combustion suppression should therefore include development of a means of accurately predicting nozzle condensation rates, although the assumption that a large proportion of metal-containing propellant additive reaches the exhaust as gas-phase species appears at present to be a reasonable one. It should also be noted that although in this paper the effects of additives are calculated on the basis of inclusion in the propellant, such incorporation is by no means the only available method of supplying a potential afterburning suppressor to the exhaust in practice.

III. Afterburning Computations

A study was made of the predicted extents of afterburning in the initially fuel-rich exhausts of double-base propellant rocket motors with different exit temperatures, total mass flow rates, concentrations of metallic propellant ingredients, and missile velocities. The study was based on a static 300 N (67 lb) thrust standard research motor operating at a chamber pressure of 3.5 MN m^{-2} (500 psi), with expansion through a conical nozzle to atmospheric pressure and a mass flow rate of 0.14 kg sec.$^{-1}$. Calculations of the exhaust flowfield were done in three stages. First, the equilibrium chemistry code NEWFEC[17] was used to calculate conditions at the nozzle throat. Next, the nonequilibrium code FIRAC[17] was used in the derivation of nozzle exit plane composition, temperature, and velocity. Computed exit plane conditions for the motor with no metallic propellant ingredients (other than lead, which unpublished experiments at the Rocket Propulsion Establishment show to have a negligible effect on radical recombination in the present context) are shown in column 2 of Table 3. The exhaust structures were calculated with a REP (Rocket Exhaust Plume) code[18, 11]. The particular code used was a simplified version of more comprehensive codes in use at the RPE, but was accurate enough for the relatively tractable conditions (negligible base recirculation region, no radial pressure gradients) of these calculations. The REP codes, which incorporate a two-equation turbulence kinetic energy mixing formulation, use an implicit numerical technique to solve the fully coupled turbulent boundary-layer and chemical rate equations. The two turbulence variables for which transport equations were solved were the turbulence kinetic energy κ and the square of a characteristic frequency of the energy-containing eddies W ($\equiv\kappa/l^2$, where l is the characteristic length scale of the turbulence). The eddy viscosity η governing the local mixing rate is given by $\rho\kappa W^{-1/2}$, where ρ is the local gas density, and among the advantages of this treatment of the mixing process over "mixing length" models is the better description of the spacial distribution of η. The REP prediction codes have been tested extensively against measurements of a variety of plume properties.[18,11]

The chemical reaction mechanisms used for nozzle and exhaust calculations are shown in Table 1, the additive reactions being added to the basic combustion mechanism as appropriate. The selection of basic combustion reactions is discussed in Refs. 11, 19-21; rate coefficients and uncertainty factors for these reactions are taken from Ref. 7. Computed exit conditions for modified propellants are shown alongside those for the unmodified propellant in Table 3. Constants for the turbulence model were as in Ref. 11.

Afterburning Criterion

It was noted in Sec. I that onset of afterburning depends upon chain branching chemical reactions producing free radicals faster than these species are removed in chain termination steps. Thus afterburning gives rise to a rapid increase in such radical concentrations as [H], typical centerline profiles for which are shown in Fig. 1. Curve 1 of Fig. 1 clearly corresponds to propagation of afterburning, for example, but curve 4 corresponds to afterburning suppression. A rather more convenient, although still somewhat arbitrary, short-hand criterion, however, is one based on the centerline distribution of temperature, because this variable is more directly related to, for example exhaust radiation levels.

Table 3 Exit plane and other input data

Quantity	Unmodified Propellant	Modified Propellants[a]	
Species Mole Fractions:			
CO	3.9×10^{-1}	3.8×10^{-1}	(6% Cl)-4.1×10^{-1} (4% Mo)
H_2	1.4×10^{-1}	1.2×10^{-1}	(6% Cl)-1.5×10^{-1} (4% Mo)
CO_2	1.3×10^{-1}	1.1×10^{-1}	(4% Mo)-1.4×10^{-1} (4% K)
H_2O	2.2×10^{-1}	2.0×10^{-1}	(4% Mo)-2.3×10^{-1} (0.1% Fe)
N_2	1.2×10^{-1}	1.1×10^{-1}	(4% K) -1.2×10^{-1} (0.1% Fe)
O_2	4.4×10^{-5}	1.0×10^{-8}	(4% K) -3.4×10^{-7} (6% Cl)
O	7.9×10^{-6}	2.1×10^{-13}	(2% Cr)-3.9×10^{-8} (6%Cl)
H	6.4×10^{-4}	5.7×10^{-7}	(2% Cr)-5.2×10^{-4} (6% Cl)
OH	8.0×10^{-6}	5.4×10^{-9}	(2% Cr)-8.6×10^{-6} (6% Cl)
PbO	2.2×10^{-3}	2.1×10^{-3}	(4% K) -2.2×10^{-3} (0.1% Fe)
KOH	–	4.5×10^{-3}	
K	–	1.9×10^{-3}	
Fe	–	3.1×10^{-4}	
FeO	–	8.1×10^{-6}	
FeOH	–	3.4×10^{-3}	
$Fe(OH)_2$	–	7.1×10^{-4}	
MoO_3	–	1.8×10^{-4}	
$HMoO_3$	–	9.8×10^{-5}	
H_2MoO_4	–	2.3×10^{-3}	
WO_3	–	6.6×10^{-6}	
HWO_3	–	6.3×10^{-5}	
H_2WO_4	–	1.3×10^{-3}	
Ba	–	4.9×10^{-8}	
BaO	–	2.6×10^{-5}	
BaOH	–	6.3×10^{-4}	
$Ba(OH)_2$	–	1.2×10^{-3}	
(Sn)	–	2.1×10^{-3}	
(Cr)	–	4.8×10^{-3}	
HCl	–	1.4×10^{-2}	
Cl	–	4.5×10^{-5}	
Cl_2	–	3.2×10^{-9}	
Temperature, K	1215	1100 (4% K)-1245 (6% Cl)	
Jet velocity, km sec^{-1}	2.06	1.92 (4% K)-2.06 (0.1% Fe)	
Jet radius, mm	9.65	9.65	
Freestream temperature, K	288	288	
Freestream velocity, km sec^{-1}	0-0.3	0-0.6	
Ambient pressure	1 atm	1 atm	

[a]The figures in parentheses refer to the particular case for which the quantity is quoted. Additive species concentrations listed are for 1% by weight of additive in the propellant, except for chlorine (2%).

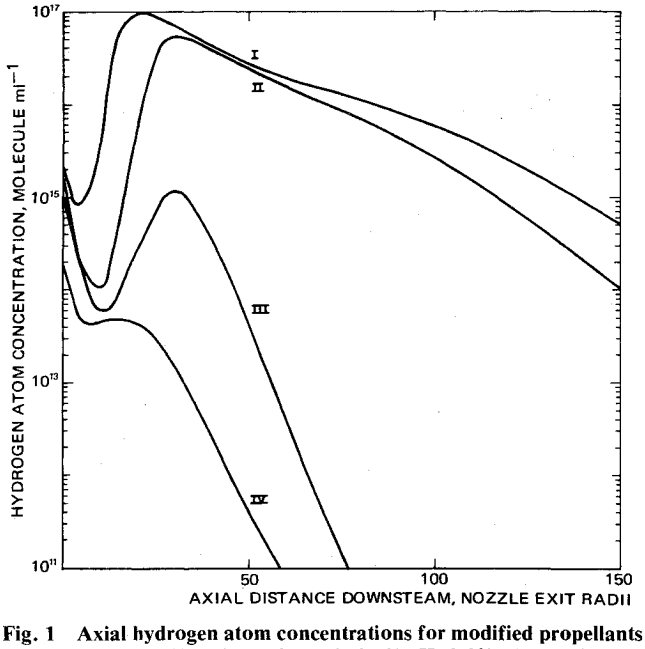

Fig. 1 Axial hydrogen atom concentrations for modified propellants containing 0.1-1.0% of iron. Curve I, 0.1%; II, 0.3%; III, 0.4%' IV, 1.0% Fe. Static conditions.

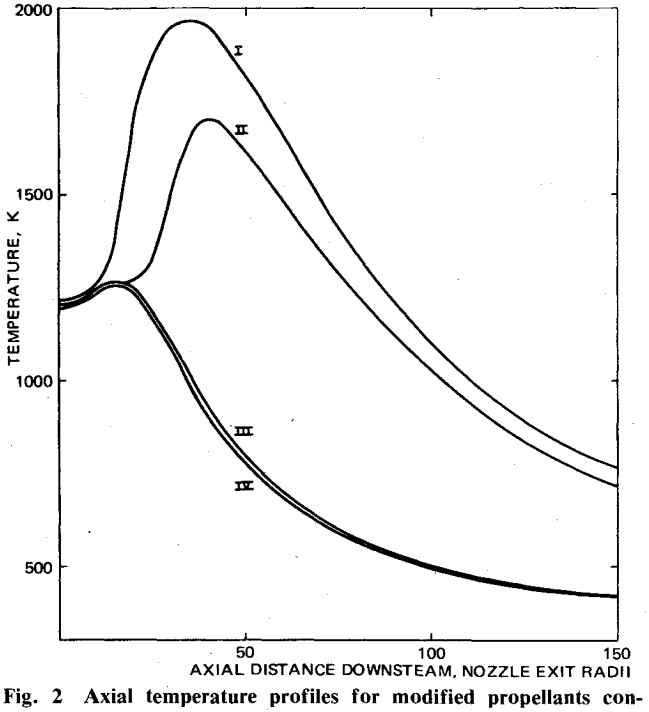

Fig. 2 Axial temperature profiles for modified propellants containing 0.1-1.0% of iron. Curve I, 0.1%; II, 0.3%; III, 0.4%; IV, 1.0% Fe. Static conditions.

Use of the temperature-distribution criterion is illustrated in Fig. 2. The same conclusion as to whether or not afterburning occurs would be reached from inspection of either Fig. 1 or Fig. 2 for these sea-level conditions (cf. Ref. 20, however, for higher altitudes).

IV. Results of Computations

Effect of Exit Temperature

The computed exhaust centerline temperature profile for the standard conditions is shown in Fig. 3, line I, which indicates a rise in temperature to a peak value of almost 2,000 K from the exit plane temperature of 1,215 K. As the exit temperature is lowered, all other conditions remaining constant, the degree of secondary burning falls off, the peak temperature reached for an exit temperature of 600 K being less than 900 K (Fig. 3, line IV). While it is not reasonable in practice to contemplate lowering the exit temperature without concomitant changes in other variables, the tendency for the extent of afterburning to decrease as this temperature falls is clear.

Effect of Mass Flow Rate (Jet Radius)

Computed distributions of axial temperatures for the standard total mass flow rate of 0.14 kg sec^{-1} and for reduced total mass flow rates (reduced exit radii) at otherwise standard conditions are shown in Fig. 4, the mass flow rate per unit exit area being held constant throughout. It is apparent that the extent of afterburning decreases as the total mass flow rate (exit radius) is lowered. For purposes of comparison, axial temperature profiles at different total mass flow rates, for the propellant modified by addition of 2% by weight of potassium as carbonate, are shown in Fig. 5; comparison of Figs. 4 and 5 indicates that for the motor used, afterburning suppression by potassium is predicted to require less additive as the total mass flow rate is decreased.

Effects of Additive Concentrations

Axial temperature profiles for different propellant concentrations of potassium (0.1-4.0% by weight as potassium carbonate) are shown in Fig. 6. This figure indicates that some 3.5% of potassium is needed to suppress afterburning for the standard motor. This prediction is subject to rather large error bounds imposed by uncertainties in the chemical kinetic input data, however; Fig. 7, for example, shows that if k_7 and k_8 take the upper limiting values indicated by Table 1 ($k_7 \times 30$ and $k_8 \times 30$, respectively), afterburning is completely suppressed by 1% of potassium. Further work on accurate determination of k_7 especially is needed, although it is worth

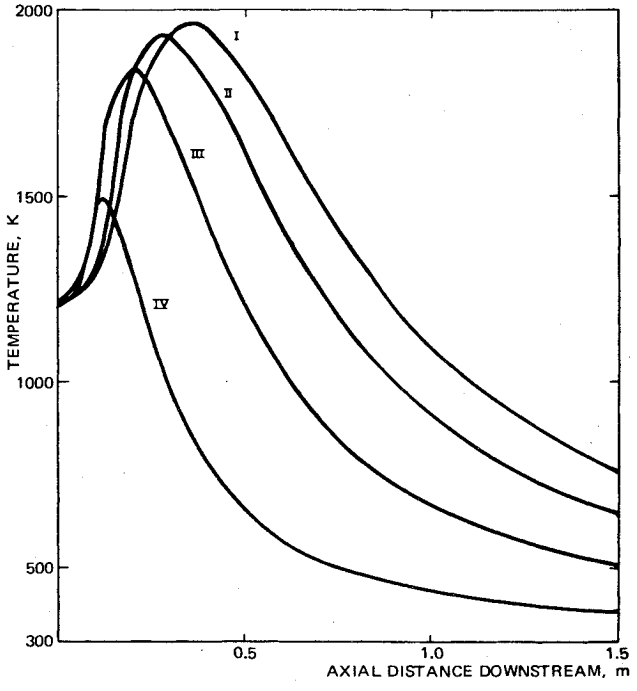

Fig. 4 Axial temperature profiles for unmodified propellant at different mass flow rates. Curve I, standard mass flow rate of 0.141 kg sec^{-1}; II, 0.094 kg sec^{-1}; III, 0.047 kg sec^{-1}; IV, 0.014 kg sec^{-1}. Static conditions.

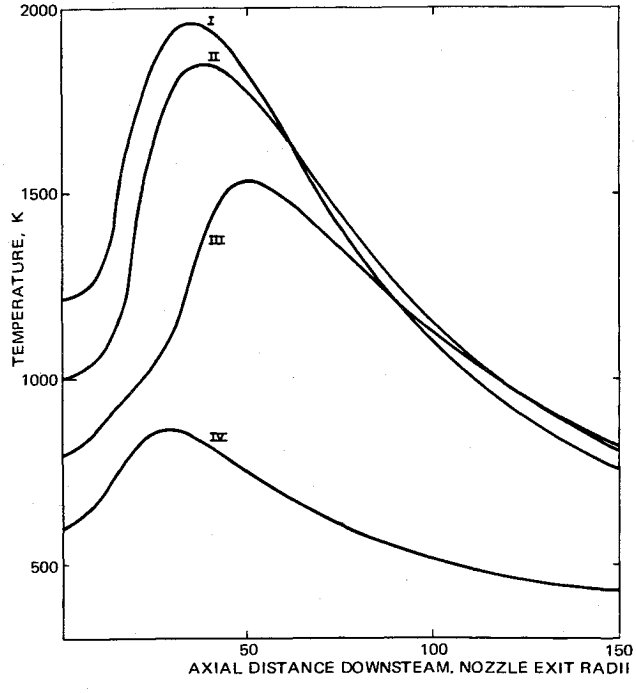

Fig. 3 Axial temperature profiles for unmodified propellant. Curve I reference, $T_e = 1{,}200$ K; II, $T_e = 1{,}000$ K; III, $T_e = 800$ K; IV, $T_e = 600$ K. Static conditions.

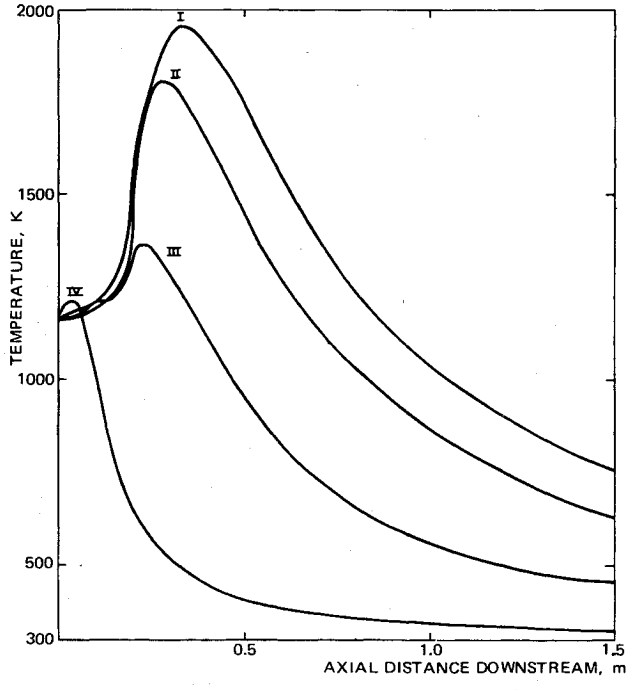

Fig. 5 Axial temperature profiles for modified propellants containing 2% of potassium as carbonate at different mass flow rates. Curve I, standard mass flow rate of 0.141 kg sec^{-1}; II, 0.094 kg sec^{-1}; III, 0.047 kg sec^{-1}; IV, 0.014 kg sec^{-1}. Static conditions.

noting that predictions and measurements for this type of motor agree with one another within the error limits of theory and experiment (cf. also Ref. 8).

The effects of iron-containing additives upon afterburning are illustrated in Fig. 2. This figure shows that as the Fe content of the propellant is increased, a sharp transition from afterburning to no afterburning takes place with a change in iron concentration from 0.3 to 0.4% by weight. The minimum weight % of iron predicted to suppress afterburning is lower than that for potassium, but more accurate chemical rate data will be required if this prediction is to be put on a firmer basis. The effect of changes in exit temperature upon afterburning of the Fe-modified propellant motor was also studied; if the exit temperature for the propellant containing 0.4% of iron is increased from 1,200 to 1,400 K, the secondary flame is predicted to reappear, while a reduction of exit temperature to 900 K results in predicted flame suppression for 0.3% of iron (see Fig. 8).

Table 4 illustrates the large deviations from chemical equilibrium encountered in this work, and emphasizes the need for accurate chemical kinetic data in calculations of this type; almost all the reactions of Table 4 show substantial departures from balance between forward and backward steps.

Under the standard conditions, about 3% by weight of molybdenum in the propellant is required to suppress afterburning; 2% gave rise to marginal combustion (maximum

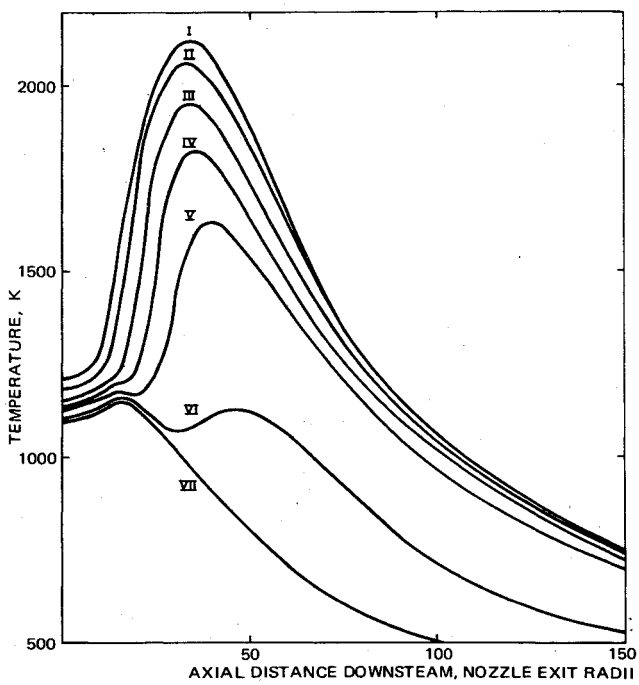

Fig. 6 Axial temperature profiles for modified propellants containing 0.1-4.0% of potassium as carbonate. Curve I, 0.1%; II, 1.0%; III, 2.0%; IV, 2.5%; V, 3.0%; VI, 3.5%; VII, 4.0%. Static conditions.

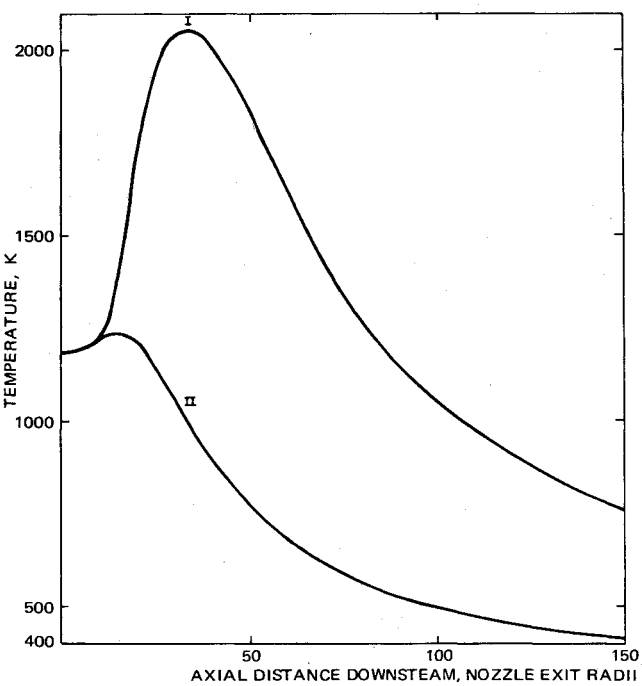

Fig. 7 Axial temperature profiles for modified propellants containing 1.0% of potassium as carbonate. Curve I, unadjusted rate coefficients; II, k_7, k_8 at upper limits (Table 1). Static conditions.

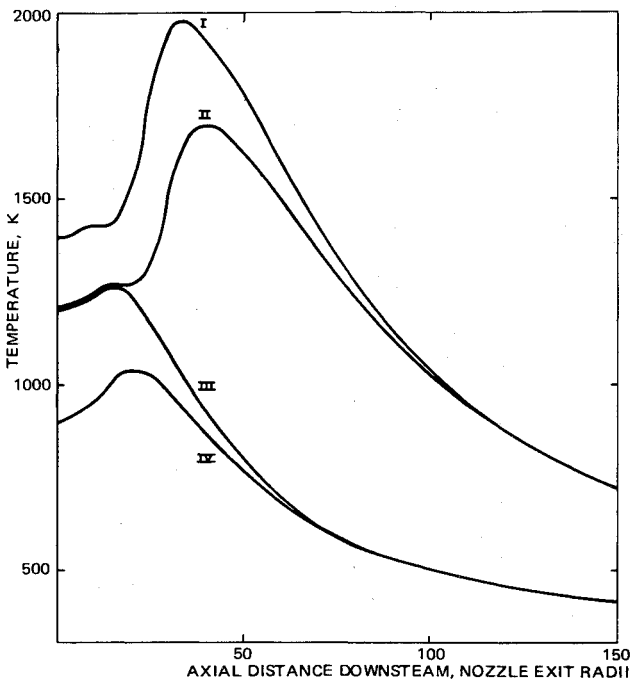

Fig. 8 Axial temperature profiles for iron-modified propellants. Curve I, 0.4% Fe, T_e=1,400 K; II, 0.3% Fe, reference curve, T_e =1,200 K; III, 0.4% Fe, reference curve, T_e = 1,200 K; IV, 0.3% Fe, T_e = 900 K.

Table 4 Local reaction rates with afterburning suppressed by iron

Reaction	Forward Rate	Backward Rate
$O+O+M \rightarrow O_2+M$	6.76×10^{12}	6.25×10^{5}
$O+H+M \rightarrow OH+M$	1.01×10^{13}	2.35×10^{2}
$H+H+M \rightarrow H_2+M$	7.53×10^{13}	1.79×10^{8}
$H+OH+M \rightarrow H_2O+M$	4.60×10^{13}	4.69×10^{6}
$CO+O+M \rightarrow CO_2+M$	2.26×10^{17}	4.12×10^{4}
$OH+H_2 \rightarrow H_2O+H$	2.89×10^{18}	1.24×10^{17}
$O+H_2 \rightarrow OH+H$	1.41×10^{18}	1.38×10^{13}
$H+O_2 \rightarrow OH+O$	1.94×10^{18}	4.90×10^{14}
$CO+OH \rightarrow CO_2+H$	1.41×10^{18}	1.11×10^{16}
$OH+OH \rightarrow H_2O+O$	3.86×10^{13}	1.69×10^{17}
$Fe+H_2O \rightarrow FeOH+H$	1.37×10^{16}	1.71×10^{17}
$FeOH+H \rightarrow FeO+H_2$	3.03×10^{18}	2.32×10^{17}
$FeO+H_2O \rightarrow Fe(OH)_2$	2.82×10^{18}	1.23×10^{14}
$Fe(OH)_2+H \rightarrow FeOH+H_2O$	4.24×10^{18}	3.02×10^{18}

Rates, in molecule ml^{-1} sec^{-1}, at an axial distance downstream of approximately 0.3 m (31 exit radii) for propellant with 1% Fe added. Static conditions. Local temperature 1,075 K.

centerline temperature about 1,600 K), and 4% extinguished the secondary flame altogether. Addition of 5% by weight of tungsten to the propellant led to a prediction of marginal afterburning ($T_{max} \approx 1{,}550$ K) and addition of 6% of tungsten to afterburning suppression. Thus both Mo and W appear to be less promising suppression candidates than Fe, although further work on the details of the mechanisms for all three additives is needed for accurate predictions.[3,4]

Addition of 2% by weight of barium to the propellant was predicted to result in suppression of afterburning, but secondary combustion was propagated with 1% of Ba added. Thus, barium is predicted to be a somewhat less effective additive than iron even on a molar basis under these conditions, again with the reservations imposed by the uncertainties in chemical rate input data. These uncertainties are larger still for chromium and tin. The results for chromium indicated that secondary combustion was suppressed when 2% by weight of chromium was added to the propellant but not for an additive level of 1%. Those for tin showed that even 5% of this metal did not prevent propagation of secondary combustion, and that tin therefore appears not to be a useful prospective afterburning suppressant under these conditions.

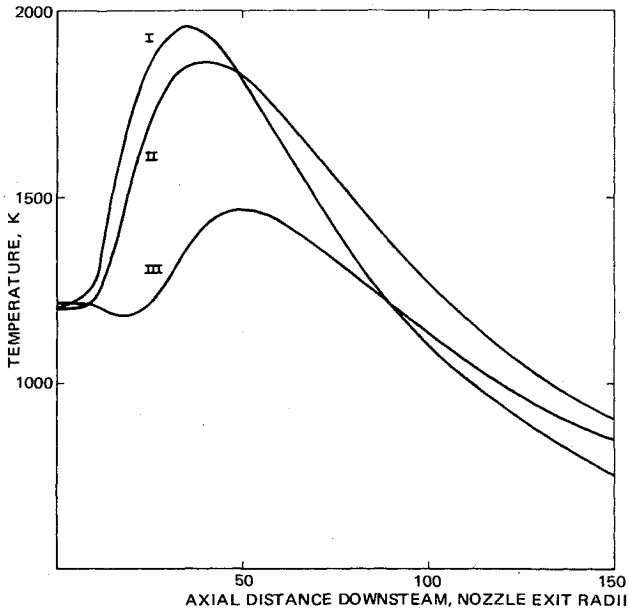

Fig. 9 Axial temperature profiles for unmodified propellant under static and subsonic flight conditions and for a modified propellant containing 0.1% iron at a flight velocity of 600 msec^{-1}. Curve I, unmodified, static; II, unmodified at 300 msec^{-1}; III, 0.1% Fe at 600 msec^{-1}.

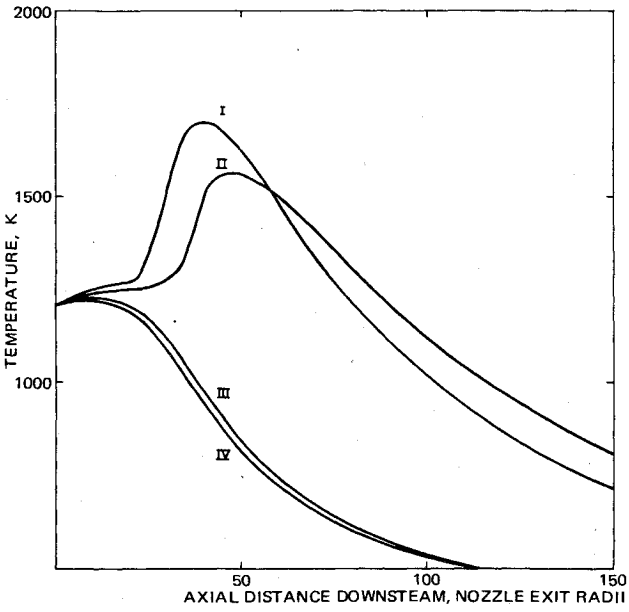

Fig. 10 Axial temperature profiles for a modified propellant containing 0.3% iron at flight velocities up to 300 msec^{-1}. Curve I, static; II, 100 msec^{-1}; III, 200 msec^{-1}; IV, 300 msec^{-1}.

The calculations for propellant with chlorine showed that this non-metal is ineffective in suppressing afterburning by comparison with several of the metallic additives under these conditions, with even 6% by weight of chlorine failing to eliminate the secondary flame.

A table listing relative efficiencies of the different additives in suppressing afterburning is deliberately not included, partly because of uncertainties in the kinetic input data, but also because a selection of suppressant for a particular motor will depend upon various factors (e.g., compatibility in the propellant, ballistic considerations, etc.), in addition to those of afterburning inhibition activity.

Effect of Missile Velocity

Axial temperature profiles for the standard motor for static conditions and for a missile velocity of 300 msec^{-1} (Mach 0.88) are compared in Fig. 9, which illustrates the tendency for the thermal plume to become longer, but the peak axial temperature lower, as the flight velocity is increased. Corresponding profiles at 0, 100, 200, and 300 msec^{-1} for the propellant with 0.3% by weight of iron are shown in Fig. 10. Under static conditions and at 100 msec^{-1} afterburning occurs, but at 200 and 300 msec^{-1} this combustion is suppresed. At 600 msec^{-1} as little as 0.1% of iron almost extinguishes the secondary flame (Fig. 9). Thus, the likelihood of afterburning occurring decreases with increasing missile velocity for these conditions.

V. Conclusions

Calculations of the exhaust properties of low-thrust rocket motors with double base propellants show that there are good prospects of controlling afterburning in these exhausts with small quantities of other metallic propellant additives as well as the traditionally used potassium. Elimination of afterburning is favored by 1) lowering the exit temperature, 2) increasing the proportion of additive in the propellant, 3) increasing missile velocity, and 4) decreasing exit radius at constant mass flow rate per unit exit area. Because onset of afterburning is essentially chemical rate-controlled, more accurate measurements of many of the rate coefficients involved are needed. Further work on condensation rates of the metal derivatives in nozzles is required. An in-house program of experimental work designed to test the predictions is in progress.

References

[1] Cotton, D. H. and Jenkins, D. R., "Catalysis of Radical Recombination Reactions in Flames by Alkaline Earth Metals," *Transactions of the Faraday Society*, Vol. 67, 1971, pp. 730-739.

[2] Bulewicz, E. M. and Padley, P. J., "Catalytic Effect of Metal Additives on Free Radical Recombination Rates in $H_2+O_2+N_2$ Flames," Thirteenth Symposium on Combustion, Combustion Institute, Pittsburgh, Pa., 1971, pp. 73-79.

[3] Jensen, D. E. and Jones, G. A., "Catalysis of Radical Recombination in Flames by Iron," *Journal of Chemical Physics*, Vol. 60, May 1974, pp. 3,421-3,425.

[4] Jensen, D. E. and Jones, G. A., "Mass Spectrometric Tracer and Photometric Studies of Catalysed Radical Recombination in Flames," *Journal of the Chemical Society, Faraday Transactions I*, Vol. 71, 1975, pp. 149-160.

[5] Rosser, W.A., Inami, S.H., and Wise, H., "The Effect of Metal Salts on Premixed Hydrocarbon-Air Flames," *Combustion and Flame*, Vol. 7, No. 2, 1963, pp. 107-119.

[6] Friedman, R. and Levy, H., "Inhibition of Opposed-Jet Methane-Air Flames," *Combustion and Flame*, Vol. 7, No. 2, 1963, pp. 195-201.

[7] Jensen, D. E. and Jones, G. A., "Gas-Phase Reaction Rate Coefficients for Rocketry Applications," unpublished data, Ministry of Defence, Great Britain.

[8] McHale, E. T., "Flame Inhibition by Potassium Compounds," *Combustion and Flame,* Vol. 24, April 1975, pp. 277-279.

[9] Stull, D. R. and Prophet, H., eds, "JANAF Thermochemical Tables, 2nd ed," NSRDS-NBS 37, June 1971, Joint Army Navy Air Force.

[10] Jensen, D. E. and Jones, G. A., "Iron Compounds in Flames," *Journal of the Chemical Society, Faraday Transactions I,* Vol. 69, 1973, pp. 1,448-1,454.

[11] Jensen, D. E. and Wilson, A. S., "Prediction of Rocket Exhaust Flame Structures," *Combustion and Flame,* Vol. 25, 1975, pp. 43-55.

[12] Kalff, P. and Alkemade, C. T. J., "Determination of Dissociation Energies for some Alkaline Earth (hydro-) Oxides in CO/N_2O Flames," *Journal of Chemical Physics,* Vol. 59, 1973, pp. 2,572-2,579.

[13] Cotton, D. H. and Jenkins, D. R., "Dissociation Energies of Gaseous Alkaline Earth Hydroxides",, *Transactions of the Faraday Society,* Vol. 64, 1968, pp. 2,988-2,997.

[14] Bulewicz, E. M. and Padley, P. J., "Photometric Observations on the Behaviour of Tin in Premixed $H_2+O_2+N_2$ Flames," *Transactions of the Faraday Society,* Vol. 67, 1971, pp. 2,337-2,347.

[15] Bulewicz, E. M. and Padley, P. J., "Photometric Observations of the Behaviour of Chromium Additives in Premixed $H_2+N_2+O_2$ Flames," *Proceedings, of the Royal Society A,* Vol. 323, June 1971, pp. 377-400.

[16] Hastie, J. W., "Molecular Basis of Flame Inhibition," *Journal of Research of the National Bureau of Standards,* Vol. 77A, 1973, pp. 733-754.

[17] Wilson, A. S., "A User's Guide to Computer Programs for the Calculation of Conditions in Flames and Rocket Nozzles," unpublished data, Ministry of Defence, Great Britain.

[18] Jensen, D. E. and Wilson, A. S., "Rapid Calculations of Physical and Chemical Structures of Rocket Exhaust Flames," Combustion Institute European Symposium (Academic Press, London and New York, 1973), pp. 723-728.

[19] Calcote, H. F. and Pergament, H. S., "Thermal and Chemi-Ionization in Afterburning Rocket Exhausts," Eleventh Symposium (International) on Combustion, The Combustion Institute, Pittsburgh, Pa., 1967, pp. 597-611.

[20] Jensen, D. E. and Pergament, H. S., "Effects of Nonequilibrium Chemistry on Electrical Properties of Solid Propellant Rocket Exhaust Plumes," *Combustion and Flame,* Vol. 17, Oct. 1971, pp. 115-124.

[21] Pergament, H. S. and Jensen, D. E., "Influence of Chemical Kinetic and Turbulent Transport Coefficients on Afterburning Rocket Plumes," *Journal of Spacecraft and Rockets,* Vol. 8, June 1971, pp. 643-649.